New Insights Into Pentosan Polysulfate Maculopathy

Michelle M. Abou-Jaoude, MD; Alexander M. Davis, BS; Claire E. Fraser, MD, PhD; Monique Leys, MD; David Hinkle, MD; J. Vernon Odom; Ramiro S. Maldonado, MD

BACKGROUND AND OBJECTIVE: To provide new insights into toxic maculopathy secondary to pentosan polysulfate (PPS) utilizing multimodal testing.

PATIENTS AND METHODS: Retrospective case-series of four patients from two academic centers evaluated with multimodal imaging, electrophysiology, dark adaptometry (DA), and genetic testing.

RESULTS: Median age was 58 years, exposure to PPS 18.5 years, and cumulative dose of 2,025 grams. Seven of eight eyes had visual acuity of 20/40 or better. Optical coherence tomography (OCT) angiography demonstrated increased choriocapillaris flow voids (54.25%) in cases compared to control (13.2%). Two subjects had abnormal foveal avascular zone configurations. Two subjects demonstrated collapse of the retinal pigment epithelium nodular excrescences and progressive retinal thinning over 4 to 5 years on OCT. Electrophysiology was normal (3/3 patients), but DA was delayed (2/2 patients).

CONCLUSIONS: The authors describe novel findings of PPS maculopathy, including flow voids in the choriocapillaris. Progressive retinal thinning may suggest a secondary retinal effect. These findings may improve understanding of the pathophysiology.

[*Ophthalmic Surg Lasers Imaging Retina.* **2021;52:xxx-xxx.**]

INTRODUCTION

Macular toxicity secondary to pentosan polysulfate (PPS) (Elmiron; Janssen Pharmaceuticals, Beerse, Belgium) was first reported in 2018.[1] PPS is the only U.S. Food and Drug Administration (FDA)-approved oral treatment for interstitial cystitis (IC), a painful urological condition[2] affecting approximately 45 in 100,000 women and eight in 100,000 men globally.[3] Pearce et al. described six patients with PPS exposure (approximately 400 mg/day, average of 15 years) presenting with pigmentary maculopathies characterized by paracentral hyperpigmentation and nodular excrescences on optical coherence tomography (OCT) at the level of the retinal pigment epithelium (RPE) with negative genetic testing.[1]

Subsequent articles investigated the strength of the association,[4] described the phenotypic range of presentation,[5,6] and generated screening recommendations.[7] Diagnostic criteria described include: 1) bilateral pathology centered on the fovea, 2) paracentral macular hyperpigmented spots, 3) dense array of hyper- and hypoautofluorescent spots and reticular fundus autofluorescence (FAF) abnormalities, and 4) foci of nodular RPE enlargement on OCT corresponding to hyperreflectance on near-infrared reflectance imaging. Humphrey visual fields (HVF) ranged from normal to dense paracentral to central scotomas correlating with the degree of atrophy[5] and analysis of electroretinography (ERG) revealed normal to diffusely dampened amplitudes.[1,4-6]

One study described findings on OCT angiography (OCTA) in a case with a choroidal neovascular mem-

From University of Kentucky College of Medicine, Department of Ophthalmology and Visual Sciences, Lexington, Kentucky (MMAJ, AMD, CEF, RSM); and Western Virginia University Eye Institute, Department of Ophthalmology, Morgantown, West Virginia (ML, DH, JVO).

Originally submitted June 29, 2020. Revision received September 19, 2020. Accepted for publication November 9, 2020.

Preliminary data presented at American Academy of Ophthalmology Genetics Club Meeting, October 2019, San Francisco, California.

Support for genetic testing from Spark Therapeutics and "My RetinaTracker" from the Foundation for Fighting Blindness. Neither source had any involvement in study design, collection, analysis, interpretation of data, manuscript writing, or the decision to submit for publication.

The authors report no relevant financial disclosures.

Address correspondence to Ramiro S. Maldonado, MD, University of Kentucky, Department of Ophthalmology, 110 Conn Terrace, Suite 550, Lexington, KY 40508; email: Ramiro.maldonado@uky.edu.

doi:

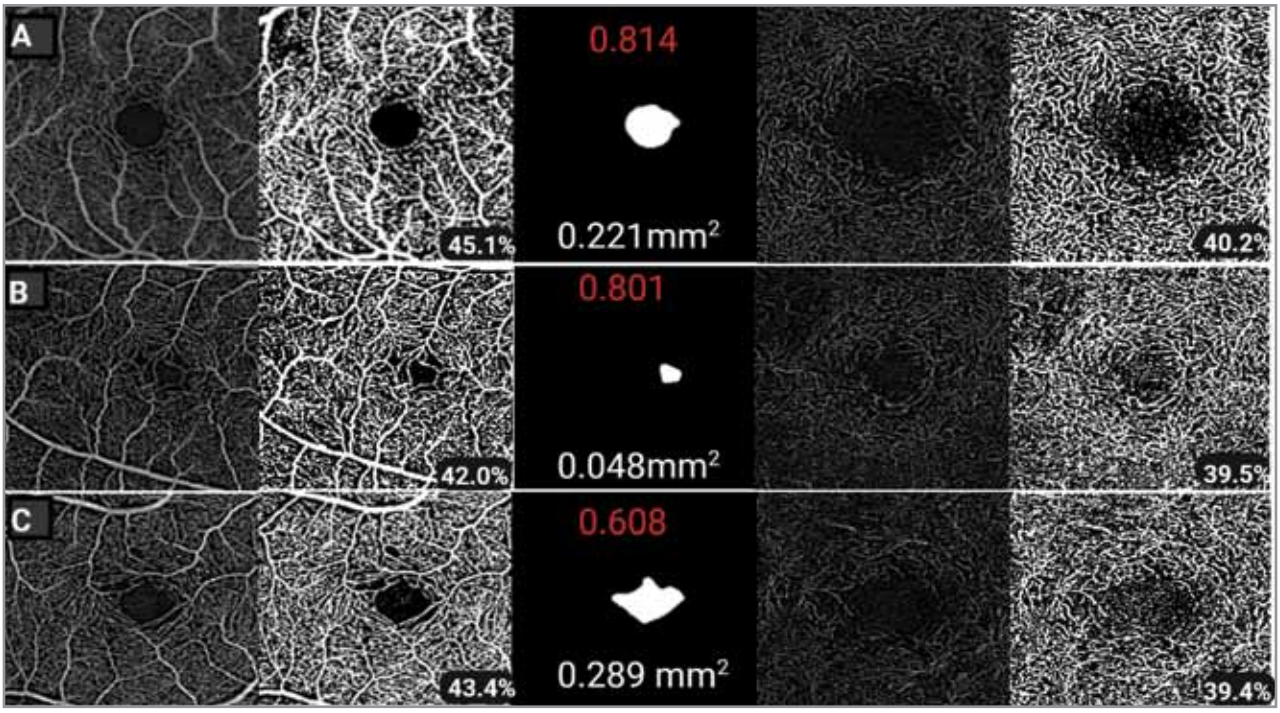

Figure 1. Optical coherence tomography angiography (OCTA) analysis of superficial and deep plexus layers with examination of the foveal avascular zone (FAZ) is shown for a normal control (row A) Patient 1 (row B), and Patient 2 (row C). From right to left: Column 1: Raw image of superficial plexus. Column 2: Superficial plexus after thresholding, vessel density shown in lower right. Column 3: Extrapolated FAZ with circularity index in red and total area in white text. Column 4: Raw image of deep plexus after removal of projection artifacts. Column 5: Deep plexus with thresholding applied, vessel density in white text. *Image quality for Patients 3 and 4 of the superficial and deep plexuses was poor; **Thresholding done with ImageJ binarization with mean thresholding algorithm.

brane,[8] and none commented on the foveal avascular zone (FAZ) or choriocapillaris layers. No studies have described electro-oculography (EOG) or quantified dark adaptometry (DA). The novel features described here may contribute to a better understanding of the pathophysiology of PPS maculopathy.

PATIENTS AND METHODS

A chart review at two academic institutions was performed. Potential cases of PPS toxicity were identified if they did not exhibit classical findings or test results of their initial diagnosis and met criteria listed by Hanif et al.[4,5] Table 1 lists patient demographics, referral diagnosis, and PPS exposure.

All patients underwent ocular examination (dilated fundus examinations, multimodal imaging, and genetic testing). Multimodal imaging included OCT and FAF using Spectralis (Heidelberg Engineering, Heidelberg, Germany). OCTA was performed for Patients 1 and 2 using the Plex Elite 9000 (Zeiss Meditec, Jena, Germany) and for Patients 3 and 4 using the Spectralis. OCTA morphometric analyses were performed with AngioTool open-source software (http://angiotool.nci.nih.gov; NIH, Bethesda, MD), with analysis of the choriocapillaris following methodology reported by Sugano et al.[9] Color thickness maps of the difference between RPE and Bruch's membrane evaluated RPE excrescence changes over time. Two authors (RM and AD) performed quality control and corrected segmentation errors manually from the automated segmentation performed on the Spectralis software (Heidelberg Eye Explorer V.1.10.0.0). The same software was utilized for total retina color thickness maps.

With appropriate genetic counseling, retinal dystrophy panels were performed: Patients 1 to 3 with a "My Retina Tracker" panel with next-generation sequencing of 266 genes (Blueprint Genetics, San Francisco, CA) and Patient 4 with inherited retinal dystrophy panel of 248 genes (Invitae, San Francisco, CA). Electrophysiology was performed following International Society for Clinical Electrophysiology of Vision protocols. The ERGs and EOGs for Patients 1 and 2 were performed using Espion E3 (Diagnosys LLC, Lowell, MA) and for Patient 4 with LKC Utas Sunburst (LKC, Gaithersburg, MD). DA was obtained in patients 1 and 2 (MonCV, Metrovision, Paris, France).

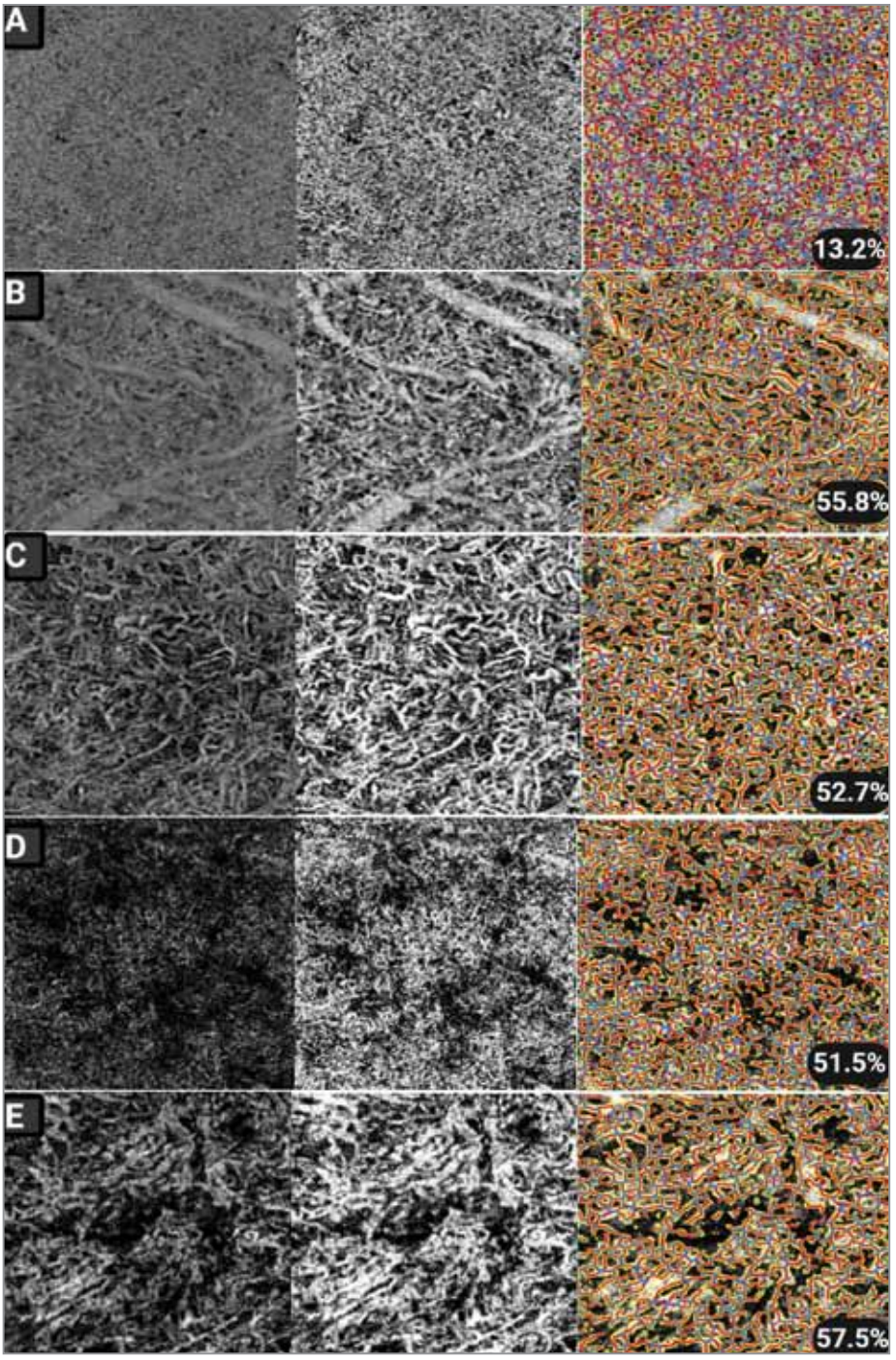

Figure 2. Optical coherence tomography angiography (OCTA) analysis of the choriocapillaris comparing a normal eye (row A) to study patients (Rows B-E). From right to left, the columns demonstrate the raw image of the choriocapillaris (Column 1), the thresholded image (Column 2), and the thresholded image with color overlay for the choriocapillaris network with the calculated flow void percentage in the bottom right (Column 3). The normal patient (A) demonstrates flow void percentages consistent with known literature, whereas the study patients (Patients 1-4 correlating with rows B-E respectively) all demonstrate significant vascular dropout and high percentage of vascular flow voids (see Table 2). *Thresholding done with AngioTool per protocol described by Sugano et al.

This research was performed in concordance with the tenets of the declaration of Helsinki and using Institutional Review Board approved protocols.

RESULTS

Four patients were evaluated. Median age was 58 years, and three of the four patients were female. Difficulty reading was the most common symptom. All carried other initial diagnoses and presenting acuities ranged from 20/20 to count fingers (CF), with seven of eight eyes having acuity better than 20/50. Genetic testing was negative for definitive mutations, although Patient 4 had three variants of unknown significance (VUS) that did not explain the phenotype (Table 2).

Patient 1 had a diagnosis of Stargardt's, but after negative genetic testing and given her exposure history, her diagnosis was subsequently changed be-

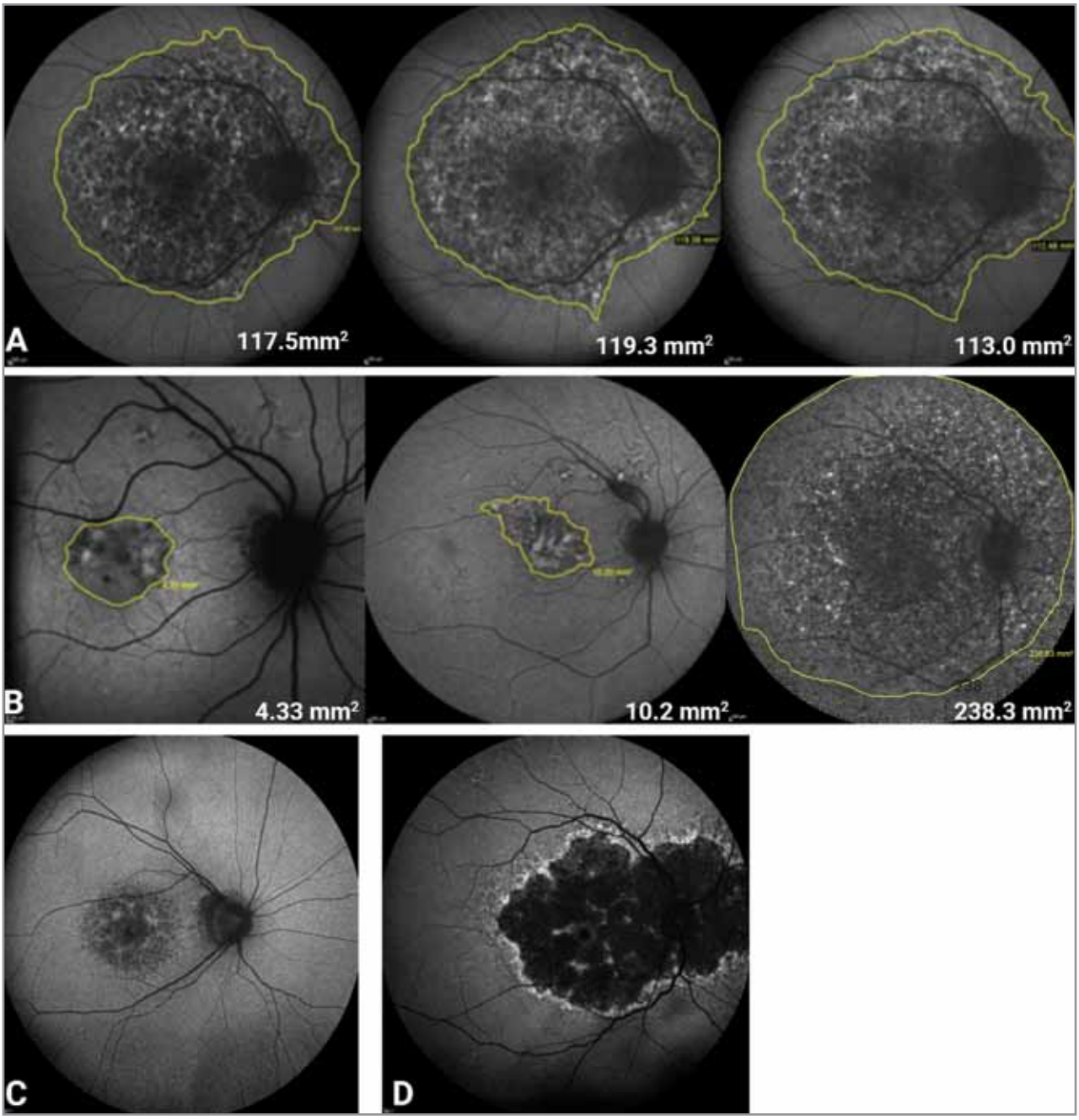

Figure 3. Fundus autofluorescence (FAF) imaging. (A) Patient 1 changes after discontinuing pentosan polysulfate (PPS). From right to left, FAF images at baseline (with 20 years of exposure), Year 3, and Year 5 demonstrating relatively stable abnormal FAF area but overall increased hyper-FAF. (B) Patient 2. From right to left, FAF images at baseline (with 15 years exposure), Year 2, and Year 4 demonstrating significant increase in abnormal FAF area over time while the patient was taking PPS. Year 3 is not shown but demonstrated similar area and autofluorescence as shown in Year 4. (C) Patient 3. Localized posterior focal RPE changes. (D) Patient 4. Diffuse atrophy centered on posterior pole with reticular/stippled edges of hyper-FAF matching the other cases.

cause although she had discontinued the PPS 4 years previously, she had a 20-year cumulative exposure and characteristic FAF. Patient 2 had both an 18-year exposure to PPS and a 10-year exposure to hydroxychloroquine (HCQ) (Plaquenil; Sanofi, Paris, France) 400 mg daily, which was discontinued 6 years before for nonspecific macular changes. Lacking the typical bull's-eye pattern of HCQ toxicity, her clinical picture was more consistent with PPS, which she was still on. Patient 3 presented with supposedly idiopathic

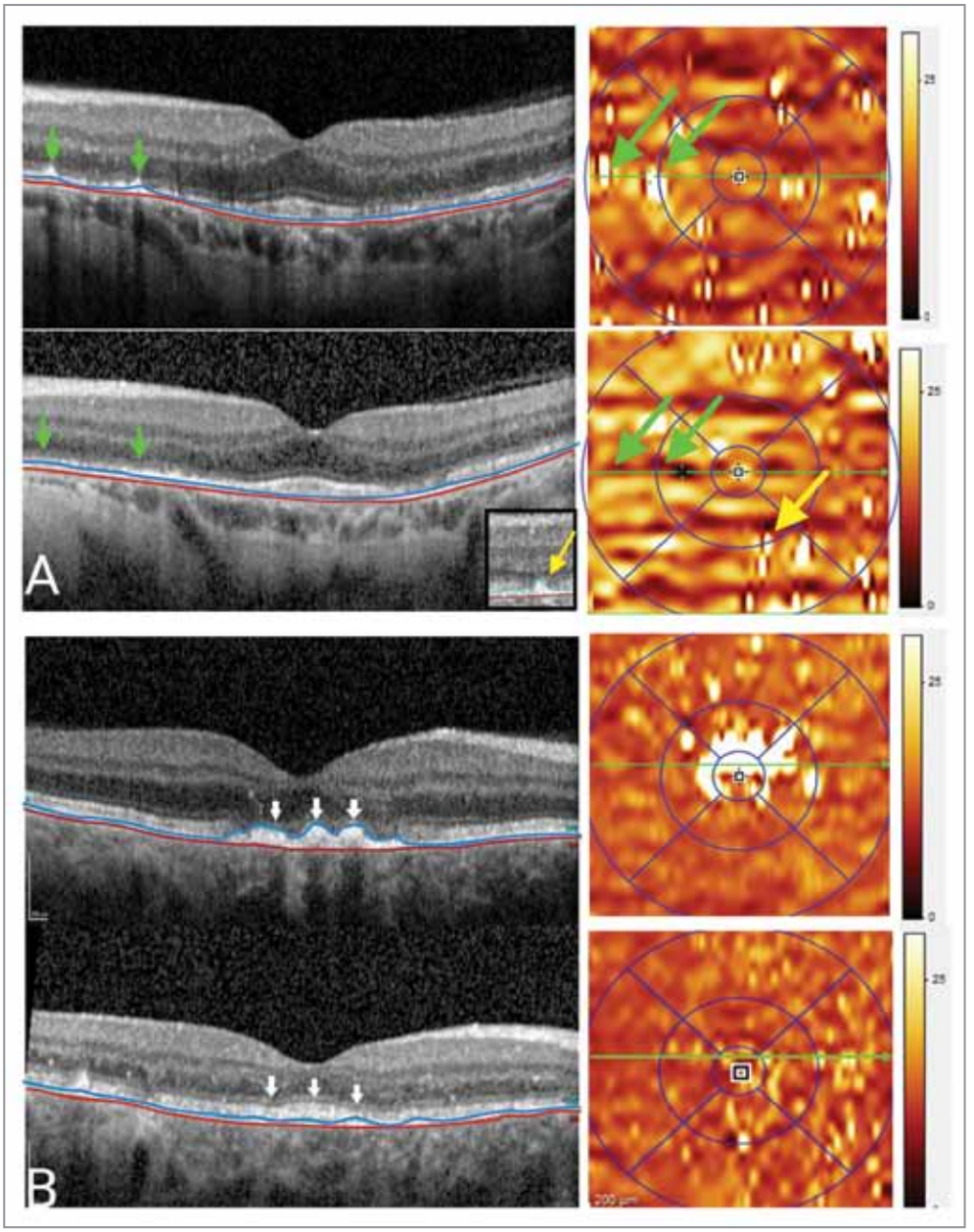

Figure 4. Retinal pigment epithelium excrescence segmentation changes over time. Each b-scan from the volumetric optical coherence tomography (OCT) was semi-automatically segmented. To the right of the b-scan is the color thickness map on a scale of 0 to 30 microns. (A) Patient 1. Initial OCT (top) and compared to 5 years later (bottom). Some excrescences collapsed (green arrows) while another appeared (yellow arrows). (B) Patient 2 initial examination (top) compared to 4 years later (bottom). Note that the focal excrescences collapse over time (white arrows) and the color map demonstrates global collapse of excrescences and presentation of new ones.

cystoid macular edema (CME) visible on fluorescein angiography (Figure A, available at www.healio.com/OSLIRetina) and had previously received intravitreal triamcinolone in the left eye. Her CME responded moderately to carbonic anhydrase inhibitors (CAIs) but with a 17-year PPS exposure and FAF findings, her diagnosis was changed to PPS toxicity. Patient 4 presented with worsening vision, a family history of age-related macular degeneration (ARMD) in his father and brother, and significant urological pathology with consequent 10-year PPS exposure. FAF findings and presentation were consistent with PPS toxicity, potentially with overlapping ARMD component.

OCTA imaging in Patients 1 and 2 demonstrated abnormal configurations of the foveal avascular zone (FAZ), including lack of circularity and one patient with an abnormally small FAZ. The vessel density was preserved at the superficial and deep plexus compared to controls (Figure 1). Choriocapillaris imaging of all patients revealed significant flow voids (average of 54.38%, standard deviation of 2.76), and choriocapillaris atrophy with visualization of large choroidal vessels (Figure 2). For reference, in normative data average flow void percentage has been reported as 14.44% (SD 4.35) in healthy patients after thresholding, consistent with our internal comparison with

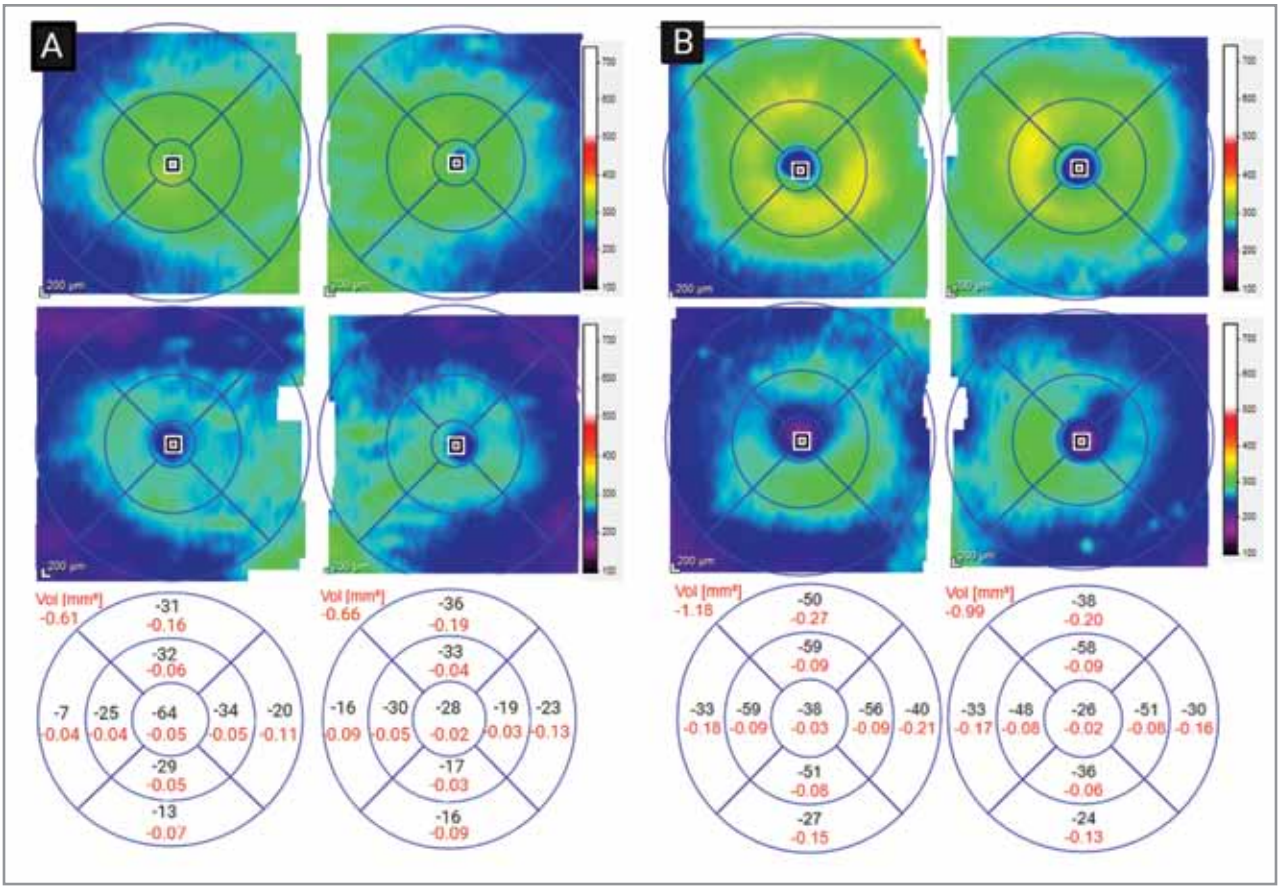

Figure 5. Total retinal thickness over time for Patients 1 (A) and 2 (B). For each, the top row is the right and left eye optical coherence tomography color map at baseline, the middle row is from the most recent visit, and the bottom row is the change in thickness for each Early Treatment Diabetic Retinopathy Study region. All four eyes demonstrate global thinning over time, including for Patient 1 after discontinuation of the medication.

a normal OCTA (flow void percentage of 13.2%) (Figure 2). Sample size was inadequate to perform statistical analysis.

All patients demonstrated varying degrees of macular pigmentary changes on fundus photography (Figure B, available at www.healio.com/OSLIRetina). FAF demonstrated a striking speckled pattern of hypo and hyperautofluorescence in Patients 1 to 3 and extensive hypoautofluorescence centered on the posterior pole and nerve in Patient 4 (Figure 3). Comparison to FAF images obtained 4 to 5 years prior demonstrated progression for Patient 1 with increased hyperautofluoresence, and for Patient 2 with increased hyperautofluoresence area.

OCT in all patients demonstrated nodular RPE abnormalities and excrescences, which in Patient 1 collapsed over time leaving ellipsoid band discontinuities without RPE atrophy (Figure 4). Patients 1 and 3 demonstrated CME, which responded to CAIs, and Patient 4 exhibited significant geographic papillomacular atrophy. Patients 1 and 2 demonstrated progressive global retinal thinning over 4 to 5 years (Figure 5), even after Patient 1 discontinued PPS 4 years prior.

Electrophysiology showed normal photopic and scotopic responses on ERG and normal Arden ratios on EOG in Patients 1 to 3 (Table 2). DA was prolonged in Patients 1 and 2 with rod-intercept time during a 30-minute period (Figure C, available at www.healio.com/OSLIRetina). Patients 1, 2, and 4 had recurrence of their bladder spasms on cessation of PPS, so significant in Patient 4 that he chose to resume the PPS and sought out other providers to dispense it.

DISCUSSION

This study provides novel information about the phenotype of PPS maculopathy. We demonstrate progression of FAF changes over 4 to 5 years (despite PPS discontinuation in one patient), collapse of nodular RPE excrescences over time, and quantification of drastic total retinal thinning in two patients during a 4- to 5-year follow-up period. We further showed

TABLE 1

Patient Demographics and Pentosan Polysulfate Exposures

Case No.	Gender	Ethnicity	Age (Years)	Urologic Diagnosis	Presenting BCVA (Snellen)	Presenting Ocular Symptoms	Diagnosis at Referral	PPS Daily Dose (mg)	Weight (kgs)	Dose by Body Weight (mg/kg)	Duration Exposure (Years)	Cumulative Dosage (g)
1	Female	White	59	IC	20/40 OD; 20/25 OS	Difficulty reading; Dark adaptation; photopsias	Stargardt disease	300*	77.11	3.9	20	2190
2	Female	White	57	IC	20/25 OU	Difficulty reading; dark adaptation; Blue photopsias	Hydroxychloroquine toxicity **	400	56.9	7.02	18	2628
3	Female	White	42	IC	20/20 OD 20/30-2 OS	Blurry vision	idiopathic CME	300	61.6	4.87	17	1862
4	Male	White	77	IC, CBPS, Kidney stones	20/40 OD; CF OS	Difficulty reading; Worsening vision OU	ARMD	300	86.1	3.48	10.3	1128
		Median	58				Median	300	14.29	4.38	17.5	2026
		Standard Deviation	14.34				Standard Deviation:	50	14.29	1.57	16.325	632.7

**Discontinued 4 years prior; **Discontinued HCQ 6 years prior due to macular changes on exam.*

IC = interstitial cystitis; CBPS = chronic bladder pain syndrome; CME = cystoid macular edema; ARMD = age-related macular degeneration; PPS = pentosan polysulfate

FAZ abnormalities and choriocapillaris dropout on OCTA, and functional quantification of the previously reported subjective DA symptoms.

The strength of this analysis is the length of follow-up with incidental multimodal imaging over 4 years. FAF findings demonstrate increasing intensity and area of characteristic changes, and OCT data show progressive macular thinning. The choroidal thickness during the same period remained stable, whether that implies a degree of direct retinal toxicity remains to be elucidated. OCT data for Patient 2 (Figure 4) demonstrated that the RPE conglomerations and excrescences are not necessarily static and can collapse over time, leaving an interrupted ez-band configuration without RPE atrophy. Hanif et al also reported this instability, noting that the RPE nodule and shape in one patient changed over a year, and another had resolution of the spots with onset of atrophy.[5] The pathophysiological implications are still unclear.

The clinical findings were consistent with the largest case series of 35 patients from Hanif et al.[5] in terms of PPS exposures, gender, RPE changes and FAF findings, possibility of CME, and negative genetic testing with normal ERGs. Another finding consistent with literature is the demonstrated progression in Patient 1 over 4 years despite cessation of PPS, also noted by Huckfeldt et al.[10] Parallel to current understanding regarding HCQ toxicity,[11,12] the progression may be reflective of progressive destabilization of damaged cells rather than the continued toxicity through a retained reservoir of PPS, but this theory is unprov-

TABLE 2

Genetic Testing, Multimodal Imaging, and Electrophysiology Findings

Case No.	OCT	FAF	OCTA Findings*	Choriocapillaris Flow Void % **	ERG Findings	Genetic Testing***	VUS	EOG Arden Ratio	DA RIT Time (min)
1	Nodular excrescences at the level of the RPE, CME	Reticular mixed hyper- and hypofluorescence centered on posterior pole bilaterally	Abnormal FAZ configuration, Flow voids at the level of the choriocapillaris	55.8	Normal	Negative	None	4.88 OD 3.11 OS	> 30
2	Nodular excrescences at the level of the RPE	Reticular mixed hyper- and hypofluorescence centered on posterior pole bilaterally	Abnormal FAZ configuration Flow voids at the level of the choriocapillaris	52.7	Normal	Negative	CNGA1 (het)	4.06 OD 4.00 OS	> 30
3	Nodular excrescences at the level of the RPE, CME	Reticular mixed hyper- and hypofluorescence centered on posterior pole bilaterally	Flow voids at the level of the choriocapillaris	51.5	Normal	Negative	None	1.67 OD 3.46 OS	N/A
4	Nodular excrescences at the level of the RPE, geographic papillomacular atrophy	Central hypoautofluorescence geographically with reticular changes at the edges	Flow voids at the level of the choriocapillaris	57.5	N/A	Negative	MYO7A (het); (pAla1541Ser), TUBCP6(het); (Silent) RP1 (het) c.2386G>A (p.Gly796Ser)	N/A	N/A
			Median	54.25					
			Standard Deviation	2.76					

** Patient 3 and 4 did not have high quality OCTA resolution of the FAZ; **On3x3 mm OCTA choriocapillaris slab; ***For Patients 1-3, testing was the 266 gene Inherited Retinal Diseases (IRD) panel; Patient 4 had 248 gene IRD panel.*

OCT = optical coherence tomography, OCTA = optical coherence tomography angiography; EOG = electro-oculogram, DA = dark adaptometry; RIT = rod-intercept time; VUS = variants of unknown significance

We demonstrated significant choriocapillaris flow voids (average of 54.38% compared with literature normative data of approximately 14%).[9] Varying degrees of choriocapillaris atrophy, as demonstrated by visualization of large choroidal vessels, may be secondary to RPE toxicity. One could also argue the reverse, given the significant degree and diffuse nature of choriocapillaris dropout compared to the relative amount of RPE atrophy. However, relative sparing of visual acuity except in cases of atrophy has been reported previously[5,6] and could support the idea that the mechanism is primary damage to the choriocapillaris, which potentially causes the RPE changes. This hypothesis is supported by the relative sparing of the inner retina and photoreceptors on OCT except in cases of advanced atrophy or edema, as all patients had significant flow voids regardless of phenotype. Two patients had abnormal FAZ configurations, which is of uncertain significance given the small sample. We hypothesize the pan-retinal thinning and decreased retinal volume may affect FAZ configuration.

The previously postulated mechanism of PPS toxicity by Greenlee et al.[13] was of RPE toxicity secondary to blockage of fibroblast growth factor (FGF) either from direct damage or the prevention of repair of damage to the RPE. The exact cellular mechanism requires further study, but the theory was based on previously noted associations of FGF with retinal organization in zebrafish[14,15] and with maintaining photoreceptor health and regeneration in response to injury.[16,17] The choroidal involvement we observed suggests either a more direct mechanism of damage to the RPE through damage to the choriocapillaris or perhaps potentiation of the proposed mechanism of FGF antagonism through additional damage to the blood-RPE barrier. Further analysis of more patients with OCTA and potentially other vascular imaging modalities is required to ascertain whether these choriocapillaris findings are as reproducible as the OCT and FAF findings. Longitudinal imaging of patients with intermediate exposures may demonstrate which changes manifest earliest and help elucidate the precise pathophysiological mechanism.

The study limitations include small sample size, and the potential for confounding factors- especially in Patient 2 with concomitant HCQ use and Patient 4 with the unknown degree of macular degeneration and the presence of genetic VUS on the *RP1* gene, resulting in a replacement of glycine with serine at codon 796. This variant has not been reported previously in patients with retinitis pigmentosa (RP), is present in population databases, in-silico tools show the resulting change to be tolerated or benign (SIFT and Polyphen, respectively) and the demonstrated phenotype was inconsistent with RP. Patient 4 also had the confounding factor of a potential ARMD component. However, compared to his similarly aged brother, the clinical picture was drastically different and the striking pattern of RPE changes implicates PPS. One might hypothesize that baseline ARMD resulted in a lower toxic threshold given that he presented with worst phenotype and atrophy with the smallest exposure (10 years). Further research is required to ascertain causation and factors associated with poorer prognoses.

These cases highlight the importance of considering alternate diagnoses when confronted with pigmentary maculopathies carrying diagnoses without proven genetic mutations or with atypical presentations. When considering medication toxicities, in patients (such as Patient 2) with multiple prolonged high-risk exposures, attention to the clinical presentations and FAF is key. Although hydroxychloroquine and PPS toxicity take years to develop and can progress despite cessation, full-blown hydroxychloroquine toxicity presents typically with a "bull's-eye" parafoveal pattern of photoreceptor loss in most Caucasian patients,[12] whereas PPS toxicity appears to manifest most apparently at the RPE with focal reticular excrescences. The potential for overlapping toxicities has not yet been explored. Both hydroxychloroquine and PPS are individually very effective in treating their respective associated conditions, and all four patients had recurrence of their IC symptoms on cessation of PPS. A detailed discussion with the patient is crucial in deciding at what level of findings to recommend cessation versus dose reduction of one or both medications.

The preponderance of evidence suggests a need for further inquiry into the association and potential screening of all patients on PPS, and the ideal timing of screening. Data are lacking in patients with intermediate exposures (between 1 and 10 years). The onset of symptoms in Patient 1 correlating with the onset of medication use, and the progressive nature over time may imply a relatively quick potential onset time with an additive effect, but further study is required especially given recent population studies without robust associations at low levels of exposure.[18]

Although the most striking findings with PPS toxicity are found with FAF, multifaceted testing may contribute to diagnosis. Potential OCTA findings are discussed above. Screening and evaluation may include questions about and measuring DA, as subjective difficulty has been reported as a significant initial finding[5] and two of two patients in this series had times greater than 30 minutes. More rapid tests validated in evaluating DA in AMD patients[19] may be fea-

sible for these patients. Because prolonged DA times are also found in AMD and other macular disorders, this may not be diagnostic but could prove helpful in supporting the diagnosis. Similarly, electrophysiological analysis such as ERG and EOG are critical to evaluating unknown maculopathies, even in the setting of PPS exposure.

CONCLUSIONS

Patients with long-term exposure to PPS may present with various pre-existing diagnoses but most PPS toxicity cases manifest with a specific constellation of OCT, FAF, and OCTA findings. Established maculopathy patients should be questioned regarding exposure to PPS, especially with negative genetic testing or atypical presentations. For patients with CME, CAIs can be effective and may need to be continued long after the PPS has been withdrawn. Patients can have progressive RPE changes even after medication discontinuation, and vascular changes may imply mechanisms of toxicity involving both the choriocapillaris and RPE. The finding of significant choriocapillaris dropout may inform understanding of the pathophysiology.

REFERENCES

1. Pearce WA, Chen R, Jain N. Pigmentary Maculopathy Associated with Chronic Exposure to Pentosan Polysulfate Sodium. *Ophthalmology*. 2018;125(11):1793-1802. https://doi.org/10.1016/j.ophtha.2018.04.026 PMID:29801663
2. Nickel JC, Moldwin R. FDA BRUDAC 2018 Criteria for Interstitial Cystitis/Bladder Pain Syndrome Clinical Trials: Future Direction for Research. *J Urol*. 2018;200(1):39-42. https://doi.org/10.1016/j.juro.2018.02.011 PMID:29452126
3. Patnaik SS, Laganà AS, Vitale SG, et al. Etiology, pathophysiology and biomarkers of interstitial cystitis/painful bladder syndrome. *Arch Gynecol Obstet*. 2017;295(6):1341-1359. https://doi.org/10.1007/s00404-017-4364-2 PMID:28391486
4. Hanif AM, Shah R, Yan J, et al. Strength of Association between Pentosan Polysulfate and a Novel Maculopathy. *Ophthalmology*. 2019;126(10):1464-1466. https://doi.org/10.1016/j.ophtha.2019.04.024 PMID:31004677
5. Hanif AM, Armenti ST, Taylor SC, et al. Phenotypic Spectrum of Pentosan Polysulfate Sodium-Associated Maculopathy: A Multicenter Study. *JAMA Ophthalmol*. 2019;137(11):1275. https://doi.org/10.1001/jamaophthalmol.2019.3392 PMID:31486843
6. Hanif AM, Yan J, Jain N. Pattern Dystrophy: An Imprecise Diagnosis in the Age of Precision Medicine. *Int Ophthalmol Clin*. 2019;59(1):173-194. https://doi.org/10.1097/IIO.0000000000000262 PMID:30585925
7. Ferguson TJ, Geraets RL, Barker MA. Chronic use of pentosan polysulfate sodium associated with risk of vision-threatening disease. *Int Urogynecol J Pelvic Floor Dysfunct*. 2019;30(3):337-338. https://doi.org/10.1007/s00192-018-3850-9 PMID:30612180
8. Mishra K, Patel TP, Singh MS. Choroidal Neovascularization Associated with Pentosan Polysulfate Toxicity. *Ophthalmol Retina*. 2020;4(1):111-113. https://doi.org/10.1016/j.oret.2019.08.006 PMID:31570285
9. Sugano Y, Sekiryu T, Furuta M, et al. Morphometrical evaluation of the choriocapillaris imaged by swept-source optical coherence tomography angiography. *Clin Ophthalmol*. 2018;12:2267-2276. https://doi.org/10.2147/OPTH.S179634 PMID:30464388
10. Huckfeldt RM, Vavvas DG. Progressive Maculopathy After Discontinuation of Pentosan Polysulfate Sodium. *Ophthalmic Surg Lasers Imaging Retina*. 2019;50(10):656-659. https://doi.org/10.3928/23258160-20191009-10 PMID:31671200
11. Marmor MF, Kellner U, Lai TYY, Lyons JS, Mieler WF; American Academy of Ophthalmology. Revised recommendations on screening for chloroquine and hydroxychloroquine retinopathy. *Ophthalmology*. 2011;118(2):415-422. https://doi.org/10.1016/j.ophtha.2010.11.017 PMID:21292109
12. Marmor MF, Kellner U, Lai TYY, Melles RB, Mieler WF; American Academy of Ophthalmology. Recommendations on Screening for Chloroquine and Hydroxychloroquine Retinopathy (2016 Revision). *Ophthalmology*. 2016;123(6):1386-1394. https://doi.org/10.1016/j.ophtha.2016.01.058 PMID:26992838
13. Greenlee T, Hom G, Conti T, Babiuch AS, Singh R. Re: Pearce et al.: Pigmentary maculopathy associated with chronic exposure to pentosan polysulfate sodium (Ophthalmology. 2018;125:1793-1802). *Ophthalmology*. 2019;126(7):e51. https://doi.org/10.1016/j.ophtha.2018.12.037 PMID:31229012
14. Vinothkumar S, Rastegar S, Takamiya M, Ertzer R, Strähle U. Sequential and cooperative action of Fgfs and Shh in the zebrafish retina. *Dev Biol*. 2008;314(1):200-214. https://doi.org/10.1016/j.ydbio.2007.11.034 PMID:18177854
15. Hernández-Bejarano M, Gestri G, Spawls L, et al. Opposing Shh and Fgf signals initiate nasotemporal patterning of the zebrafish retina. *Development*. 2015;142(22):3933-3942. https://doi.org/10.1242/dev.125120 PMID:26428010
16. Hochmann S, Kaslin J, Hans S, et al. Fgf signaling is required for photoreceptor maintenance in the adult zebrafish retina. *PLoS One*. 2012;7(1):e30365. https://doi.org/10.1371/journal.pone.0030365 PMID:22291943
17. Qin Z, Kidd AR III, Thomas JL, et al. FGF signaling regulates rod photoreceptor cell maintenance and regeneration in zebrafish. *Exp Eye Res*. 2011;93(5):726-734. https://doi.org/10.1016/j.exer.2011.09.003 PMID:21945172
18. Ludwig CA, Vail D, Callaway NF, Pasricha MV, Moshfeghi DM. Pentosan polysulfate sodium exposure and drug-induced maculopathy in commercially insured patients in the United States. *Ophthalmology*. 2020;127(4):535-543. https://doi.org/10.1016/j.ophtha.2019.10.036 PMID:31899034
19. Jackson GR, Scott IU, Kim IK, Quillen DA, Iannaccone A, Edwards JG. Diagnostic sensitivity and specificity of dark adaptometry for detection of age-related macular degeneration. *Invest Ophthalmol Vis Sci*. 2014;55(3):1427-1431. https://doi.org/10.1167/iovs.13-13745 PMID:24550363

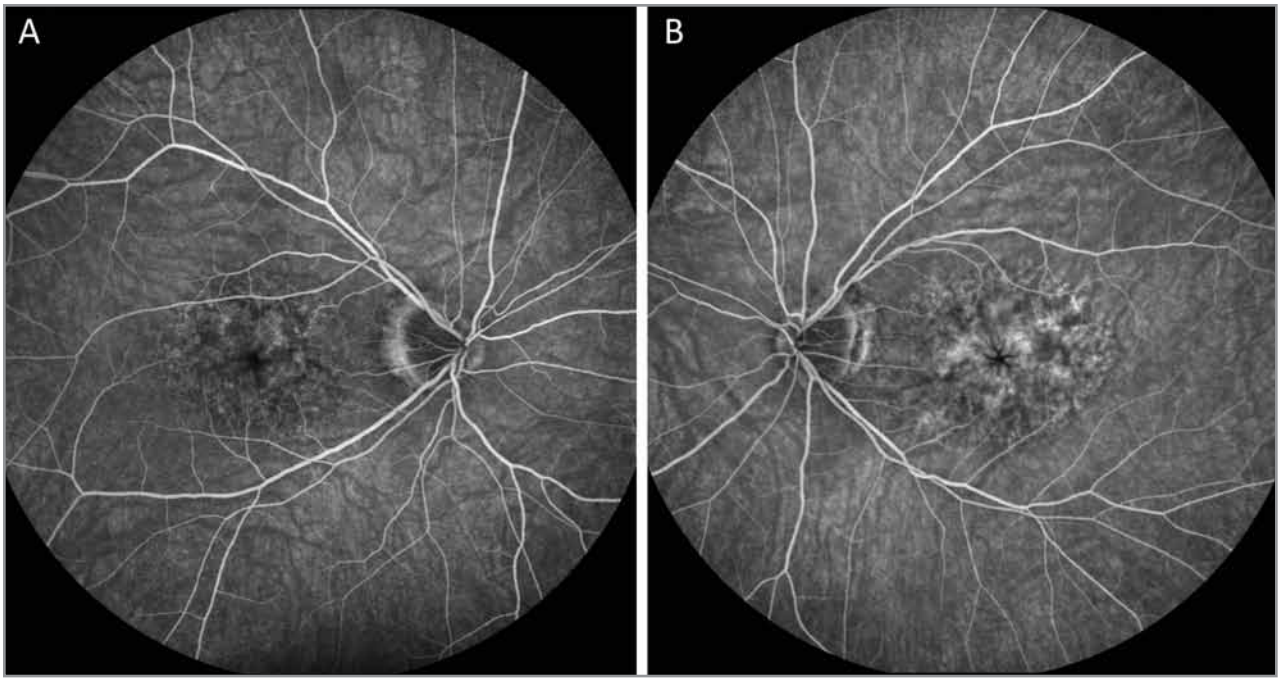

Figure A. Fluorescein angiography of Patient 3 of the right (A) and left (B) eyes demonstrating petaloid macular edema.

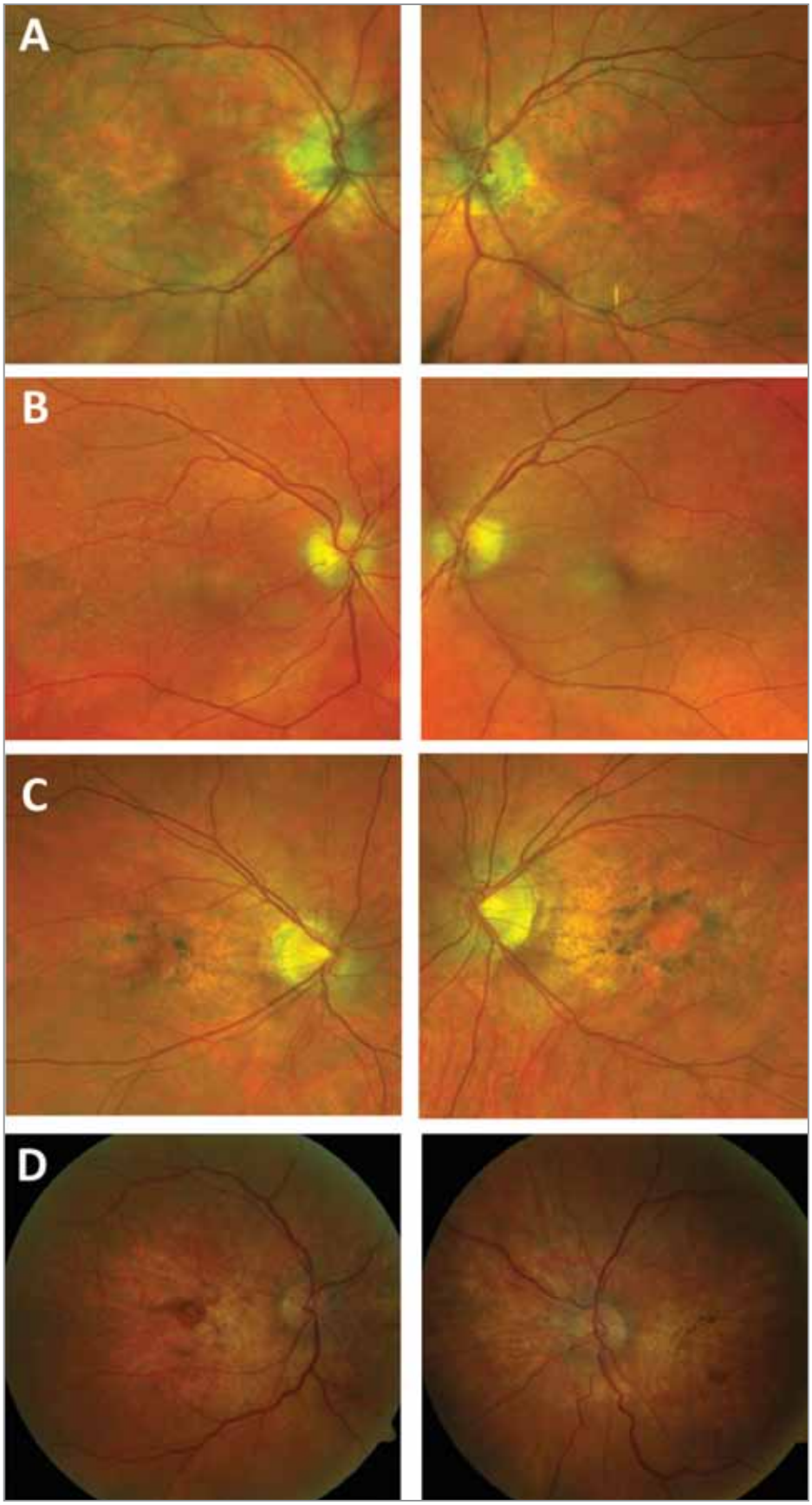

Figure B. Color fundus photos of Patients 1 through 4 in panels A to D respectively. All demonstrate retinal pigment epithelium changes centered on the macula that appear more subtle than the corresponding autofluorescence findings. Pigment clumping is especially notable in Patients 3 and 4 (C, D) and foveal changes appear consistent with underlying atrophy in Patient 4 (D).

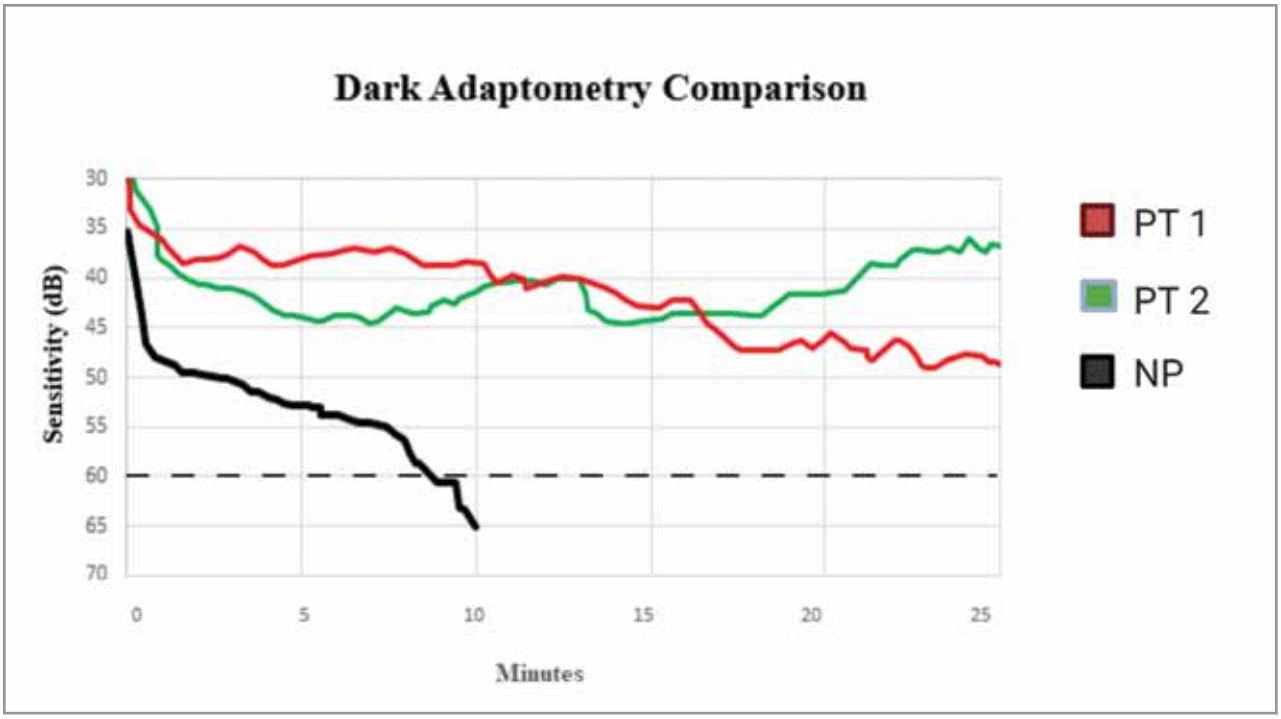

Figure C. Comparison of dark adaptometry results for Patients 1 and 2 compared with normal control. Demonstrates severely delayed dark adaptation for study patients. Rod intercept time for the normal control was 8 minutes. Patients 1 and 2 did not reach rod-intercept time at 30 minutes when testing was stopped.